Communication Using Synchronization of Optical-Feedback-Induced Chaos in Semiconductor Lasers

Y. Liu, H. F. Chen, J. M. Liu, P. Davis, and T. Aida

***Abstract*—A communication system based on the synchronization of optical chaos in semiconductor lasers is proposed. The optical chaos is generated in a single-mode semiconductor laser with external ring optical feedback. Synchronization of chaos is performed by a direct optical-injection scheme that consists of a transmitter laser with an external optical feedback and a receiver laser with optical injection from the transmitter laser. Both numerical and experimental results on synchronization of giga-hertz chaotic signals are presented. Direct encoding of 2.5 Gbps messages on the chaotic waveform is numerically demonstrated. The bit-error rate shows a sensitive dependence on the frequency detuning.**

***Index Terms*—Chaos synchronization, injection locking, optical chaos, optical communication, optical feedback.**

I. Introduction

In the last decade, chaos synchronization has been applied to communication systems over a wide range of bandwidth [1]–[5]. Synchronization of optical-feedback-induced chaos is among the first schemes proposed for applying chaos synchronization to high-frequency communication systems. Other schemes to generate chaos in semiconductor lasers include optical injection and optoelectronic feedback. Chaotic optical communications based on chaos generated by such schemes have also been considered [6]. There are a number of advantages in using chaotic signals generated in semiconductor lasers with external optical feedback: 1) An optical-feedback-induced chaotic state can have a very high dimension due to the delay-induced dynamics [7]; 2) The optical-feedback-induced chaos can achieve a high bandwidth ranging from a few giga-hertz to tens of giga-hertz; 3) The optical-feedback scheme is very simple and can be easily implemented in modules. In the past few years, several algorithms have been demonstrated to achieve synchronization of optical-feedback-induced chaos between two semiconductor lasers [8]–[12]. Recently, a direct injection scheme [13] was applied to synchronize the feedback-induced optical chaos, which uses an external cavity semiconductor laser on the transmitter side and a semiconductor laser with optical injection on the receiver side [14]. The direct injection scheme received considerable attention due to its simple configuration [15], [16]. We restrict ourselves to the direct injection scheme in this paper.

For the direct injection scheme, the complex electric fields of the transmitter laser, E^T, and the receiver laser, E^R, are respectively described by following equations:

$$\frac{dE^T(t)}{d(t)} = \frac{\Gamma}{2}\Delta G^T(N^T)E^T(t) - j\omega^T(N^T)E^T(t) + \eta_{\text{ext}}E^T(t-\tau) \quad (1)$$

$$\frac{dE^R(t)}{d(t)} = \frac{\Gamma}{2}\Delta G^R(N^R)E^R(t) - j\omega^R(N^R)E^R(t) + \eta_{\text{inj}}E^T(t-\tau_R). \quad (2)$$

Here, the superscripts T and R denote transmitter and receiver, respectively. The first equation describes the dynamics of a semiconductor laser with optical feedback with the feedback strength η_{ext} and the round trip time τ, and the second equation describes the dynamics of a semiconductor laser with optical injection from the transmitter laser with the injection strength η_{inj} and the propagation time τ_R, N represents the carrier density in the laser active layer, $\Gamma\Delta G(N)$ and $\omega(N)$ represent the carrier-dependent net optical gain and the angular frequency, respectively.

In the synchronization scheme described by these equations, there are a number of critical issues that are very important when applying the present synchronization scheme to communication systems. First, the existence of the synchronization solution is guaranteed by the equality of the feedback term and the optical injection term. However, in (1), the feedback light has exactly the same optical frequency as that of the light emitted from the laser, whereas in (2), there is usually a nonzero frequency detuning between the optical frequencies of the light in the laser and the injection light. Furthermore, for systems which use an external mirror to reflect feedback light back into the laser, depending on the feedback level, there exists the multiple reflection effect for the transmitter laser which is not included in (1), whereas such a problem does not exist for the directly injected receiver laser. Next, the coupling between the transmitter laser and the receiver laser involves both the magnitude and phase of the laser field, which are also the only externally accessible dynamical variables of a semiconductor laser.

Manuscript received February 26, 2001; revised August 11, 2001. The work of H. F. Chen and J. M. Liu is supported by the Army Research Office under Grant DAAG55-98-1-0269. This paper was recommended by Guest Editor L. Kocarev.

Y. Liu is with the ATR Adaptive Communications Research Laboratories, Seika-cho, Soraku-gun, Kyoto 619-0288, Japan, and also with the Center for Engineering Science Advanced Research, Computer Science and Mathematics Division, Oak Ridge National Laboratory, Oak Ridge, TN 37831-6355 USA (e-mail: liuy2@ornl.gov).

P. Davis, and T. Aida are with the ATR Adaptive Communications Research Laboratories, Seika-cho, Soraku-gun, Kyoto 619-0288, Japan.

H. F. Chen and J. M. Liu are with the Department of Electrical Engineering, University of California at Los Angeles, Los Angeles, CA 90095 USA.

Publisher Item Identifier S 1057-7122(01)10388-0.

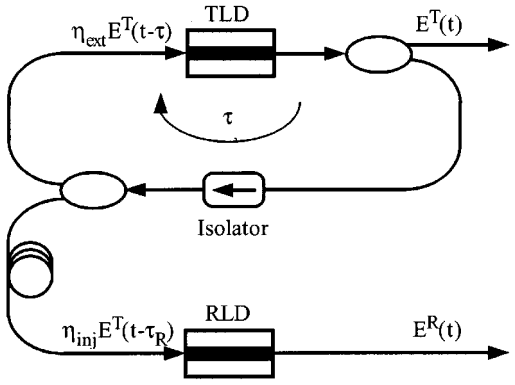

Fig. 1. Schematic of optical-chaos synchronization by optical injection.

The receiver laser output can be either a synchronized signal of the transmitter laser or simply a chaos-driven oscillation of the transmitter laser, depending on the injection condition. In both cases, the receiver laser output resembles the transmitter laser output in both waveform and spectrum. These issues have not been clearly dealt with before raising doubts on the correspondence between theory and experimental results.

In this paper, we aim at clarifying these issues for the purpose of proposing an optical communication system using the optical-feedback-induced chaos in semiconductor lasers. In the next section, we first propose an optical-feedback-induced chaos scheme using a semiconductor laser with an external ring cavity to completely avoid the multiple reflection effect. The effects of frequency detuning and injection strength on synchronization performance are investigated and the difference between the synchronized state and the driven state due to strong injection is shown. Following the numerical results, in Section III, we set up an experiment using two single-mode semiconductor lasers coupled in the direct injection scheme. Chaos synchronization in gigahertz bandwidth is experimentally demonstrated when the injection strength matches the feedback strength of the external ring cavity of the transmitter laser, thereby verifying the existence of chaos synchronization rather than the chaos-driven oscillation with the proposed scheme. Finally, in Section IV, we propose a GHz communication scheme using the synchronized optical-feedback-induced chaos. The bit-error rate (BER) for a 2.5 Gbps message is evaluated for a wide range of frequency detuning and the results demonstrate that the BER sensitively depends on the frequency detuning.

II. Chaos Synchronization and Chaos-Driven Oscillation

The configuration of our scheme for synchronizing optical-feedback-induced chaos via direct injection is shown in Fig. 1. The output light from the transmitter laser diode (TLD) is divided into two beams, one is coupled back to the transmitter laser itself with the feedback strength $\eta_{\rm ext}$ and the other is injected into the receiver–laser diode (RLD) with the injection strength $\eta_{\rm inj}$. The optical length of the external feedback path in the TLD is $l_{\rm ext}$. An optical isolator is used to avoid both multiple reflection in the feedback loop of the TLD, and mutual coupling between the TLD and the RLD. Rewriting the complex electric fields in (1) and (2) as $E(t) = A(t)\exp(-i\omega_0 t)$, one has the following equations [16]:

$$\frac{dA^T(t)}{dt} = -\frac{\gamma_c}{2}A^T(t) + i\left(\omega_0^T - \omega_c^T\right)A^T(t) + \frac{\Gamma}{2}(1-ib)g^T A^T(t) + \eta_{\rm ext}A^T(t-\tau) \times \exp(i\omega_0^T\tau) + F_{\rm sp}^T f \quad (3)$$

$$\frac{dA^R(t)}{dt} = -\frac{\gamma_c}{2}A^R(t) + i\left(\omega_0^R - \omega_c^R\right)A^R(t) + \frac{\Gamma}{2}(1-ib)g^R A^R(t) + \eta_{\rm inj}A^T(t-\tau_R) \times \exp(i\omega_0^T\tau_R - i\Omega t) + F_{\rm sp}^R \quad (4)$$

where A is the total complex intracavity field amplitude at the oscillation frequency ω_0, γ_c is the cavity decay rate, ω_c is the longitudinal mode frequency of the cold laser cavity, b is the linewidth enhancement factor, Γ is the confinement factor, $\tau = l_{\rm ext}/c$ is the delay time of the external feedback, g is the gain coefficient. $\Omega = \omega_0^T - \omega_0^R$ is the detuning frequency between TLD to RLD and τ_R is the propagation time from TLD and RLD. In this paper we assume $\tau_R = \tau$ without loss of generality. $F_{\rm sp}$ is the complex Langevin noise term that is characterized by the spontaneous emission factor $R_{\rm sp}$. The carrier density within the cavity is described by the following equation:

$$\frac{dN^{T,R}(t)}{dt} = \frac{J^{T,R}}{ed} - \gamma_s N^{T,R}(t) - \frac{2\varepsilon_0 n^2}{\hbar(\omega_0^{T,R})^2}g^{T,R}\left|A^{T,R}(t)\right|^2 \quad (5)$$

where J is the injection current density, e is the electronic charge, d is the active layer thickness, and γ_s is the carrier decay rate. The injection current density J can be normalized with a dimensionless parameter $\tilde{J} = (J/ed - \gamma_s N_0)/\gamma_s N_0$. Also, $\eta_{\rm ext}$ and $\eta_{\rm inj}$ are normalized with γ_c as $\eta_{\rm ext} = \gamma_c\xi_{\rm ext}$ and $\eta_{\rm inj} = \gamma_c\xi_{\rm inj}$, respectively. We assume identical values of b, Γ, γ_c, and γ_s for both the TLD and the RLD since these parameters have much less influence on synchronization performance than frequency detuning or injection strength [15], [16].

Numerical simulations have been conducted using the above equations. Fig. 2 shows a set of numerical results obtained at two typical injection conditions. Laser parameters are $\tilde{J}^R = \tilde{J}^T = 0.67, b = 4, \Gamma = 0.4, \gamma_c = 2.4\times10^{11}$ s^{-1}, $\gamma_s = 1.458\times10^9$ s^{-1}, and $R_{\rm sp} = 4.7\times10^{18}$ V^{2}m^{-2} s^{-1}, which are typical values for a single-mode Fabry-Perot semiconductor laser used for optical injection [17]. The top trace of Fig. 2(a) shows the chaotic intensity variation of the TLD. At this feedback level ($\tau = 3.0$ ns and $\xi_{\rm ext} = 0.01$), the transmitter laser is in a completely chaotic state as can be seen from the time series and also from the broadened peaks of its corresponding power spectrum shown in the top trace of Fig. 2(b). The middle trace of Fig. 2(a) shows the output intensity signal of the RLD at $\xi_{\rm inj} = \xi_{\rm ext}$. Because there is no parameter mismatch or noise included in the simulation, one obtains a perfectly synchronized waveform and power spectrum at the output of the RLD. The bottom trace

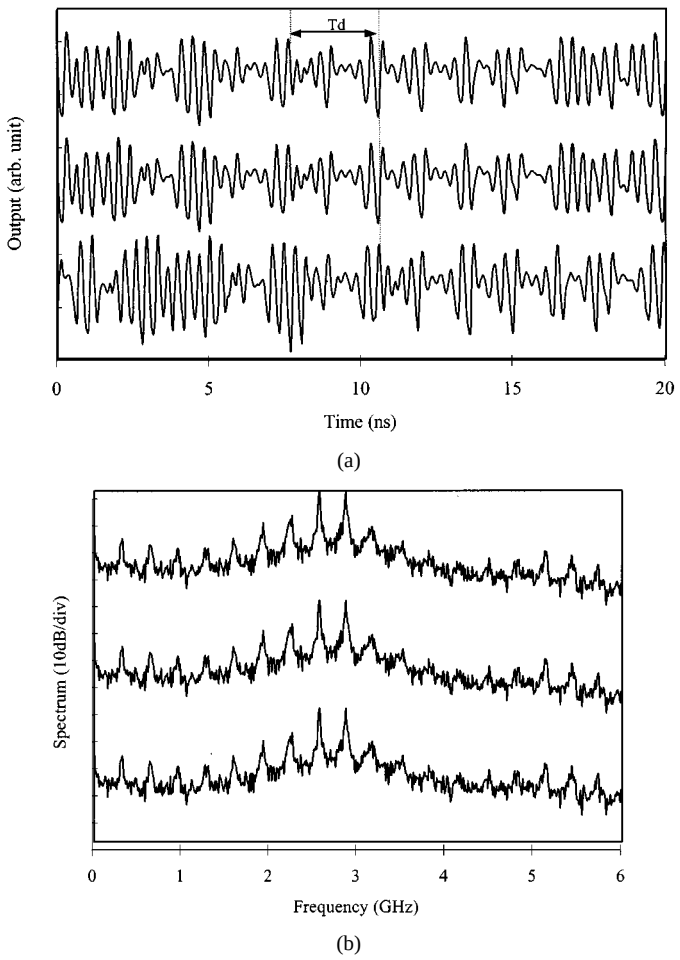

Fig. 2. (a) Time series. (b) RF spectra of laser output calculated at $\bar{J}^R = \bar{J}^T = 0.67, \tau = 3$ ns, $\xi_{\rm ext} = 0.01$, and $\Omega = 0$. Top trace: output of TLD, middle trace: output of RLD at $\xi_{\rm inj} = \xi_{\rm ext} = 0.01$, bottom trace: output of RLD at $\xi_{\rm inj} = 0.3$. All traces are plotted with same scale. Note that there is a time lag $T_d = \tau$ between the top and bottom traces.

in Fig. 2(a), however, is the time series obtained when a much stronger injection strength ($\xi_{\rm inj} = 30\xi_{\rm ext}$) is chosen. Other parameters of the RLD are assumed the same as those of the TLD. From the correlation function, we find a time lag T_d between the top trace and the bottom trace. This time lag is verified to be equal to the delay time τ. Actually, a comparison of $|E^T(t-\tau)|^2$ and $|E^R(t)|^2$ shows that they correspond extremely well except for a nonunity factor between the amplitudes of these two signals. The excellent correspondence between the top and bottom traces can also be seen in the power spectra of the two signals [Fig. 2(b)]. In other words, in the case of strong injection, by linearly transforming and shifting the output of the RLD, one can get an almost identical signal as the output of the TLD.

Let us briefly comment on the significance of the time lag T_d due to the strong injection ($\xi_{\rm inj} \gg \xi_{\rm ext}$). For perfect synchronization with no frequency detuning, because $\tau_R = \tau$ is assumed in the simulation, the output of the RLD, $E^R(t)$, is identical to the output of the TLD, $E^T(t)$, i.e., $E^R(t) = E^T(t)$, while receiving the injection signal $E^T(t-\tau)$ from the TLD. In other words, in the case of perfect synchronization, the RLD reproduces the dynamics of the TLD. In contrast, in the case of strong injection, the RLD behaves more like a driven oscillator

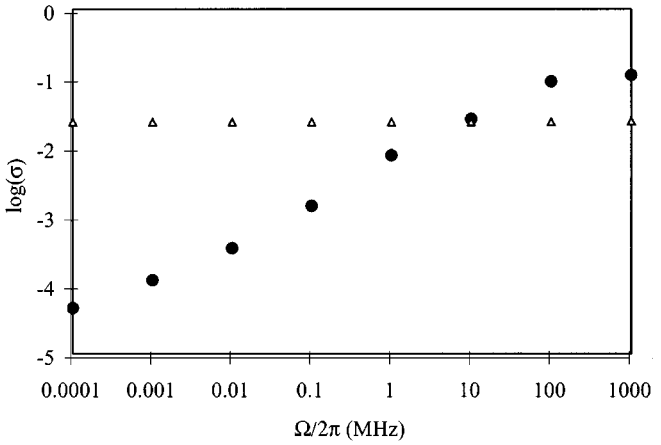

Fig. 3. Synchronization error (σ) versus detuning frequency. Black dots: $\xi_{\rm inj} = \xi_{\rm ext} = 0.01$, triangles: $\xi_{\rm inj} = 30\xi_{\rm ext} = 0.3$. Other parameters are the same as in Fig. 2.

with its output directly responding to the injection signal, i.e., $E^R(t) \propto E^T(t-\tau)$. It has been shown in previous works [15], [16] that, in the case of synchronization, the time lag between the output waveforms of the receiver and transmitter laser is determined by the difference between the propagation time and the delay time of the ring cavity, i.e., $T_d = \tau_R - \tau$; while in the case of driven oscillation, the time lag is only determined by the propagation time, i.e., $T_d = \tau_R$. Though very similar optical and RF spectra between the two lasers may be observed in both cases, the absence or presence of a time lag tells the difference between the two scenarios.

To quantitatively evaluate the synchronization performance, we define a general synchronization error as $\sigma = \langle |f(S^R(t) - S^T(t)| \rangle / \langle S^T(t) \rangle$ where $\langle\ \rangle$ denotes the time average and f denotes a function consisting of a time shift and a linear transformation to normalize the amplitude of the RLD output signal to that of the TLD. Fig. 3 shows the synchronization error σ as a function of the detuning frequency for both synchronization and driven-oscillation cases. For the synchronization case, the synchronization error has a minimum value at $\Omega = 0$ and increases as a power function of Ω. On the other hand, for the case when the receiver laser behaves as a driven oscillator, there is no remarkable change in the synchronization error when the frequency detuning varies.

III. Experimental Results of Chaos Synchronization

Experiments on synchronization were performed using a setup schematically shown in Fig. 4. Here, we use a DFB semiconductor laser with external optical feedback as the transmitter to generate chaotic signal and another DFB laser subject to the optical injection from the transmitter laser as the receiver. Even when the laser output is chaotic, the side-mode suppression ratios of both lasers are measured to be about 40 dB, which guarantees the single-mode operation of both lasers. The injection current of the laser is set at 12.4 mA which is about 1.67 times of the laser threshold current (7.41 mA) of the free-running laser. At this operation point, the wavelength is 1537.49 nm and the relaxation oscillation frequency is measured to be 3.3 GHz. The wavelength and the relaxation

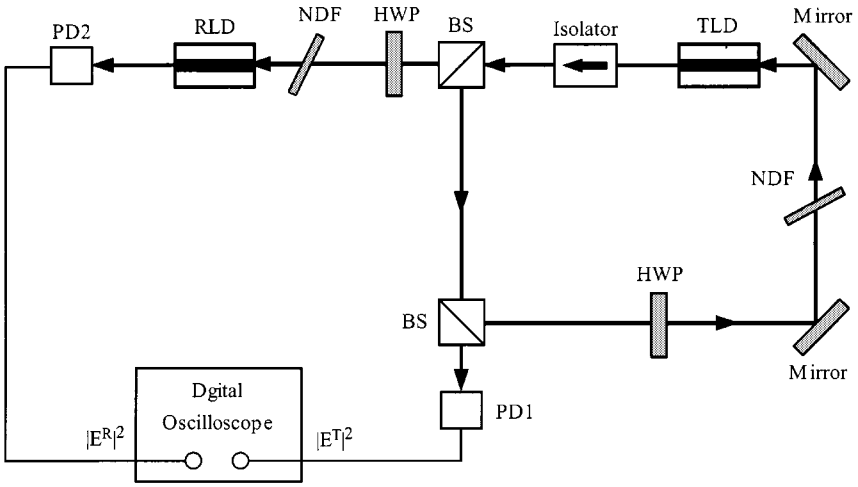

Fig. 4. Experimental setup for synchronization. PD: photodiode, NDF: neutral density filter, BS: beam splitter, HWP: half-wave plate.

oscillation frequency of the receiver laser are matched to those of the transmitter laser by adjusting the injection current and the operation temperature (both within the accuracy of 1%). By monitoring the beat signal between two free-running lasers, we can set the frequency detuning between the two lasers within a few megahertz. The intensity variations of the laser output is detected by a photoreceiver of 6 GHz bandwidth and is observed with a digital oscilloscope of 3 GHz bandwidth and 10 Gbit/s sampling rate as well as a RF spectral analyzer of 8-GHz bandwidth.

An optical isolator with an isolation of 60 dB is used to avoid both multiple reflection in the feedback loop of the TLD and mutual coupling between the TLD and the RLD in the experiment. Half-wave plates are used to adjust the polarization states of the feedback/injection light in order to obtain the maximum feedback/injection effects. The time delay of the external ring cavity length is measured to be 3.3 ns. The feedback level, as well as the injection strength, is varied with neutral density filters. In the current experiment, the feedback level is controlled within the range of $\xi_{\text{ext}} = 0.005 \sim 0.1$. By gradually increasing the feedback level, we observed a continuous bifurcation from periodic oscillation to quasiperiodic oscillation, and finally to chaos. The oscillation frequencies of the periodic states and the spectral peak frequency of the chaotic oscillation vary from a few gigahertz to more than 10 GHz depending on the injection current level of the laser. In this experiment, we limit the bias injection current to a low level to set the relaxation oscillation frequency around 3 GHz, which is within the bandwidth of the digital oscilloscope, so that the temporal variations of the chaotic waveform can be observed with sufficient resolution.

Fig. 5(a) shows a typical chaotic time series of the transmitter laser output (upper trace) and the receiver laser output (bottom trace) obtained in the experiment. The corresponding power spectra are shown in Fig. 5(b). The broadening of the spectral peaks indicates chaotic variations of times series while the discrete peaks show beat frequencies corresponding to the external ring cavity. The maximum spectral peak is at 3.34 GHz. A good correspondence between the output waveforms of the two lasers can be recognized from both the time series and the spectra. We calculated the synchronization error to be about 10% in Fig. 5.

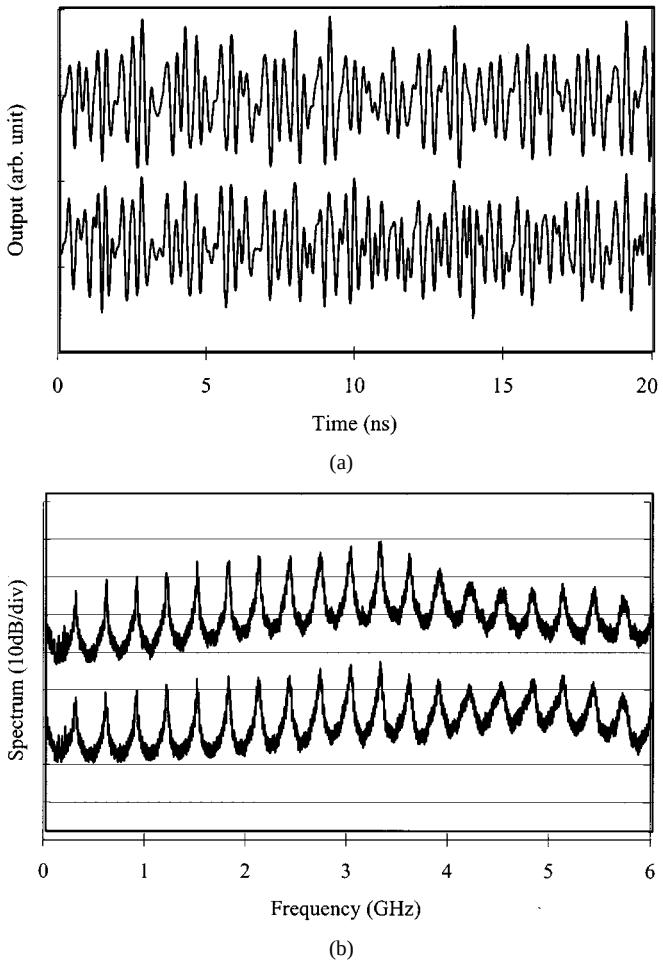

Fig. 5. Experimental results of synchronization: (a) Time series. (b) RF spectra. Upper trace output of TLD, lower trace output of RLD.

As explained in the previous section, a tricky problem in this synchronization scheme is the difference between synchronization and driven oscillation. Since for both cases RLD output has a waveform similar to that of TLD, it is difficult to distinguish the two cases from the optical or RF spectra of the two lasers. We have checked the time relationship and have verified that the time lag between the RLD and the TLD decreases as τ is in-

creased. We have further verified that the synchronization error rapidly deteriorates when the injection strength deviates from the optimum value. These evidences strongly suggest that the observed phenomenon is indeed the synchronization rather than the chaos-driven oscillation. The details of the experiment will be published elsewhere.

IV. Communication Schemes Using Optical-Feedback-Induced Chaos

A number of message-encoding methods have been applied to optical-feedback-induced chaos for cryptographic communications. One method used a chaos shift keying algorithm by modulating the injection current of the transmitter laser with a bit sequence to switch the transmitter laser output between two different chaotic attractors corresponding to "1" and "0" bits [9], [18]. At the receiver end, two lasers are prepared which synchronize respectively to the attractors of "1" and "0" bits. Message recovery is performed by detecting the difference between a receiver laser output signal and the injection light signal. The disadvantage of this method is that the bit frequency is limited by the synchronization time and accordingly a high bit rate cannot be expected. The second method employed a chaos masking scheme by superimposing a small modulated optical signal onto the light output of the transmitter laser or by adding a small modulated electric signal to the transmitter laser injection current. Message decoding at the receiver end is performed by taking the difference between the receiver laser output signal and the injection light signal. This method was implemented in several experiments [2], [10], [12]. A recent experiment reported that it is possible to mask a sinusoidal signal up to the relaxation frequency of the laser [12]. This simple method is, however, less efficient because only a part of the injection light power carries information, most being used to mask information. A third method directly encodes the information onto the chaotic signals within the feedback loop of the transmitter laser. The message-encoded signal is also used to synchronize the receiver laser. This method was applied to a number of optical-chaos systems [19]–[22]. The main advantage of this method is that it does not require that the encoded message be at a lower frequency compared to the chaotic carrier signal. In this paper, we apply this method to our synchronization scheme. We numerically show that perfect chaos synchronization can still be achieved for a certain range of modulation depth and, as a result, a reasonable BER performance can be obtained for a high bit rate of 2.5 Gpbs.

Fig. 6 shows a schematic of message encoding in our chaos synchronization system. Here, an electro-optical modulator is inserted in the external feedback loop of the transmitter laser. Using this modulator, we modulate the optical field as $m(t)E^T(t)$, where $m = 1+\chi$ for a "1" bit, and $m = 1-\chi$ for a "0" bit. Here, $\chi < 1$ is the modulation amplitude. When adding the messages, the feedback term in (3) and the injection term in (4) are changed to $\eta_{\text{ext}} m(t)A^T(t-\tau)$ and $\eta_{\text{inj}} m(t)A^T(t-\tau_R)$, respectively. One can easily find that the inclusion of the message does not change the symmetry between the transmitter and the receiver lasers. We verified this through numerical simulations. To show how the modulation amplitude, i.e., the message amplitude, affects the synchronization quality, we change the value of χ and calculate the

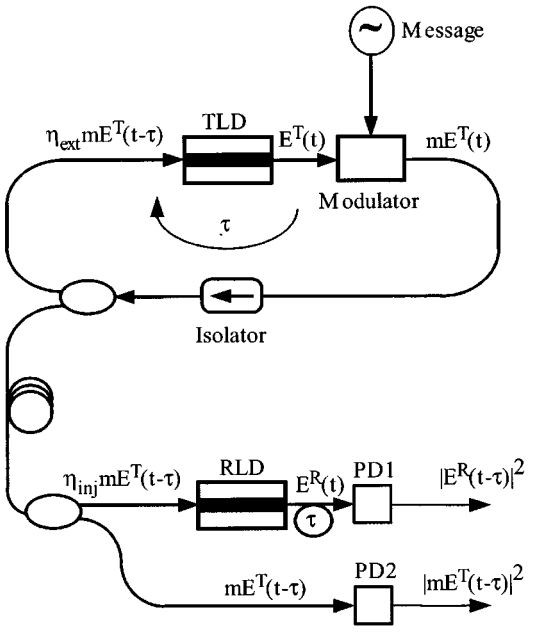

Fig. 6. Schematic of optical communication scheme using synchronization of optical-induced-chaos. $\tau_R = \tau$ was assumed.

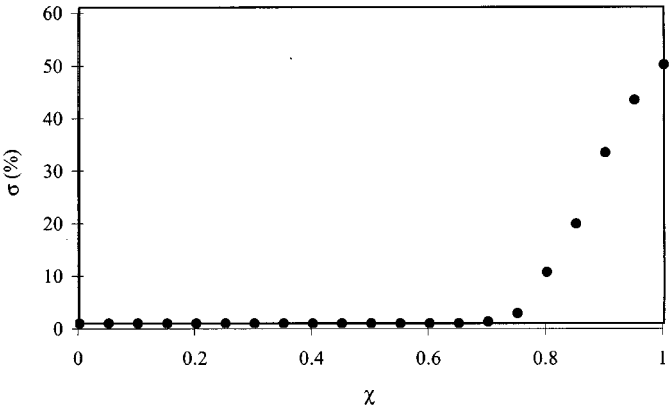

Fig. 7. Calculated synchronization error versus modulation amplitude χ. Parameters are: $\bar{J}^R = \bar{J}^T = 0.67, \tau = 3$ ns, $\xi_{\text{inj}} = \xi_{\text{ext}} = 0.01$. The message is a pseudo-random NRZ code at a bit rate of 2.5 Gbps.

synchronization error σ. Fig. 7 shows the variation of σ as a function of χ. Here, a nonreturn-to-zero (NRZ) pseudo-random bit sequence was employed as the message. From Fig. 7, we find that perfect synchronization between the TLD and the RLD is achieved for a wide range of the modulation amplitude. This is essentially different from another optical chaos system [8] where a nonsymmetrical configuration between TLD and RLD was employed.

At the receiver end in Fig. 6, the light output of the RLD is detected by a photo-receiver and generates an electrical signal proportional to $|E^R(t)|^2$. Meanwhile, a part of the injection light from the TLD is directly detected by the second photo-receiver and generates the signal proportional to $|m(t)E^T(t)|^2$. When the RLD is synchronized to the TLD, the encoded message can be recovered from the ratio of $|E^T(t)|^2$ and $|E^R(t)|^2$ as $\tilde{m}^2 = |E^T(t)|^2/|E^R(t)|^2$. It is noted that the above recovery algorithm is based on the condition that the light output of the RLD is not a driven signal, but a synchronized signal

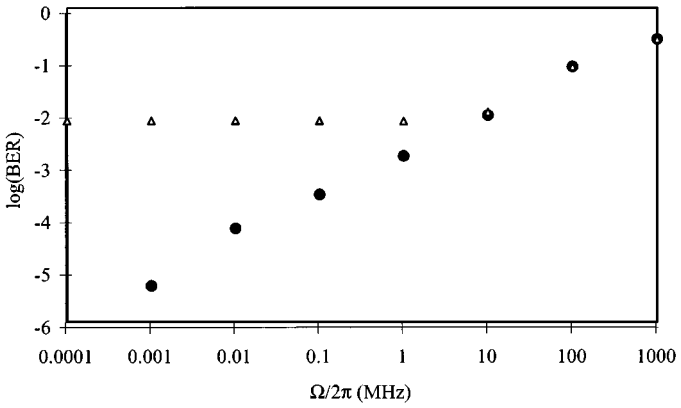

Fig. 8. Calculated BER versus frequency detuning. Parameters are: $\bar{J}^R = \bar{J}^T = 0.67, \tau = 3$ ns, $\xi_{\rm inj} = \xi_{\rm ext} = 0.01$. Black dots: no noise, triangles: noise at SNR $= 40$ dB. The message is a pseudo-random NRZ code at a bit rate of 2.5 Gbps with the modulation factor of $\chi = 0.15$.

of the TLD. In other words, the RLD receives the signal of $mE^T(t-\tau)$, while it synchronizes to the signal $E^T(t)$.

To study the performance of this system, we encode a pseudo-random NRZ bit sequence and calculate the BER. Fig. 8 shows the BER as a function of the frequency detuning for a message with the bit rate of 2.5 Gbps and $\chi = 0.15$. Here, $\tilde{m}$ is evaluated from the ratio $|E^T(t)|/|E^R(t)|$ and no averaging was performed. BER is computed using the bit length up to 10^7 bits. Note that both the BER and the frequency detuning are plotted in logarithmic scale. There is a linear relationship between the variations of log (BER) and log Ω, which is similar to the case of the synchronization error shown in Fig. 3. The BER in the presence of noise is plotted in triangle marks in Fig. 8 for comparison. The noise factor is evaluated with the signal-to-noise ratio (SNR) which is defined as SNR $= 20\log(\langle|E^T(t)|\rangle/\langle|\zeta(t)|\rangle)$ where $\langle|\zeta(t)|\rangle$ is the average noise amplitude [22]. SNR was evaluated to be about 40 dB at this case. Improvement of BER can be expected with the reduction of noise level.

The bit rate of the encoded message is limited only by the main frequency of chaotic signal. In this particular example, a 2.5 Gbps bit rate was chosen due to the fact that a relatively low injection current of the laser was used which results in the laser relaxation frequency below 3 GHz. Higher bit rate up to 10 GHz can be achieved by using a laser operated at higher injection current.

There is a trade-off between the BER and the secrecy of the message. A large modulation depth can improve the BER, but at the same time, the message has the risk of being exposed in the transmitted signal. For the encoding condition used in obtaining Fig. 8, we have checked the transmitted signal $m(t)E^T(t)$ and have verified that the message cannot be taken directly from time series of the transmitted signal. In fact, even the bit repetition frequency cannot be recognized from the power spectrum of the transmitted signal.

V. Conclusion

An optical communication system based on the synchronization of optical-feedback-induced chaos in two semiconductor lasers is proposed and studied. Synchronization is achieved by directly injecting the light output from the transmitter laser to the receiver laser. We have demonstrated that, depending on the injection condition and the frequency detuning between the transmitter and receiver lasers, the receiver laser can be in either the synchronization state or the driven-oscillation state. Though in both states the oscillation characteristics of the receiver laser are similar to those of the transmitter laser, these two different states can be distinguished from the temporal relationship between the output waveforms of the two lasers and from the limited tolerance of the synchronization state to parameter mismatch between the two lasers. Experimentally, an external ring cavity was used to generate optical chaos in the transmitter laser and a direct optical injection was used to synchronize two lasers. Synchronization of giga-hertz chaotic signals was demonstrated with this experimental setup. It was shown with numerical simulations that message encoding can be performed in the present chaos synchronization system by directly modulating the transmitter laser output. A pseudo-random NRZ sequence with the bit rate of 2.5 Gbps is successfully recovered when chaos synchronization is achieved. The BER was evaluated and a very sensitive dependence of the BER on the frequency detuning between two lasers was demonstrated through the numerical simulation.

Acknowledgment

The authors are grateful to B. Komiyama for encouragement and support, and Y. Takiguchi for valuable experimental help.

References

[1] L. M. Pecora and T. L. Carroll, "Synchronization in chaotic systems," *Phys. Rev. Lett.*, vol. 64, no. 8, pp. 821–824, 1990.
[2] K. M. Cuomo and A. V. Oppenheim, "Circuit implementation of synchronized chaos with applications to communications," *Phys. Rev. Lett.*, vol. 71, no. 1, pp. 65–68, 1993.
[3] G. D. Van Wiggeren and R. Roy, "Communication with chaotic lasers," *Science*, vol. 279, pp. 1198–1200, 1998.
[4] J. P. Goedgebuer, L. Larger, and H. Porte, "Optical cryptosystem based on synchronization of hyperchaos generated by a delayed feedback tunable laser diode," *Phys. Rev. Lett.*, vol. 80, no. 10, pp. 2249–2252, 1998.
[5] Y. Liu, P. Davis, and T. Aida, "Synchronized chaotic mode hopping in DBR lasers with delayed opto-electronic feedback," *IEEE J. Quantum Electron.*, vol. 37, pp. 337–352, Mar. 2001.
[6] J. M. Liu, H. F. Chen, and S. Tang, "Optical Communication Systems Based on Chaos in Semiconductor Lasers," *IEEE Trans. Circuits Syst. I*, vol. 48, pp. 1475–1483, Dec. 2001.
[7] K. Ikeda and K. Matsumoto, "High-dimensional chaotic behavior in systems with time-delayed feedback," *Physica D*, vol. 29, pp. 223–235, 1987.
[8] C. R. Mirasso, P. Colet, and P. Garcia-Fernandez, "Synchronization of chaotic semiconductor lasers: Application to encoded communications," *IEEE Photonics Tech. Lett.*, vol. 8, no. 2, pp. 299–301, Feb. 1996.
[9] V. Annovazzi-Lodi, S. Donati, and A. Sciré, "Synchronization of chaotic lasers by optical feedback for cryptographic applications," *IEEE J. Quantum Electron.*, vol. 33, no. 9, pp. 1449–1454, Sept. 1997.
[10] S. Sivaprakasam and K. Shore, "Demonstration of optical synchronization of chaotic external-cavity laser diodes," *Opt. Lett.*, vol. 24, no. 7, pp. 466–468, 1999.
[11] Y. Takiguchi, H. Fujino, and J. Ohtsubo, "Experimental synchronization of chaotic oscillations in externally injected semiconductor lasers in low-frequency fluctuation regime," *Opt. Lett.*, vol. 24, no. 22, pp. 1570–1572, 1999.
[12] I. Fischer, Y. Liu, and P. Davis, "Synchronization of chaotic semiconductor laser dynamics on subnanosecond timescales and its potential for chaos communication," *Phys. Rev. A*, vol. 62, no. 1, pp. 011 801-1–011 801-4, 2000.

[13] A. R. Volkovskii and N. F. Rulkov, "Synchronous chaotic response of a nonlinear oscillator system as a principle for the detection of the information component of chaos," *Tech. Phys. Lett.*, vol. 19, no. 2, pp. 97–99, 1993.
[14] J. K. White and J. V. Moloney, "Synchronization and communication with chaotic semiconductor lasers," in *Proc. NOLTA'97*, 1997, pp. 129–132.
[15] V. Ahlers, U. Parlitz, and W. Lauterborn, "Hyperchaotic dynamics and synchronization of external-cavity semiconductor lasers," *Phys. Rev. E*, vol. 58, no. 6, pp. 7208–7213, 1998.
[16] Y. Liu, H. F. Chen, J. M. Liu, P. Davis, and T. Aida, "Synchronization of optical-feedback-induced chaos in semiconductor lasers by optical injection," *Phys. Rev. A*, vol. 63, no. 3, pp. 031 802-1–031 802-4, 2001.
[17] J. M. Liu and T. B. Simpson, "Four-wave mixing and optical modulation in a semiconductor laser," *IEEE J. Quantum Electron.*, vol. 30, no. 4, pp. 957–965, Apr. 1994.
[18] J. K. White and J. V. Moloney, "Multichannel communiation using an infinite dimensional spatiotemporal chaotic system," *Phys. Rev. A*, vol. 59, no. 3, pp. 2422–2426, 1999.
[19] G. D. Van Wiggeren and R. Roy, "Optical communication with chaotic waveforms," *Phys. Rev. Lett.*, vol. 81, no. 16, pp. 3547–3550, 1998.
[20] L. G. Luo, P. L. Chu, and H. F. Liu, "1-GHz optical communication system using chaos in erbium-doped fiber lasers," *IEEE Photonics Tech. Lett.*, vol. 12, pp. 269–271, Mar. 2000.
[21] P. Colet and R. Roy, "Digital communication with synchronized chaotic lasers," *Opt. Lett.*, vol. 19, no. 24, pp. 2056–2058, 1994.
[22] C. T. Lewis, H. D. I. Abarbanel, M. B. Kennel, M. Buhl, and L. Illing, "Synchronization of chaotic oscillations in doped fiber ring lasers," *Phys. Rev. E*, vol. 63, no. 1, pp. 016 215-1–016 215-15, 2001.

Y. Liu, photograph and biography not available at the time of publication.

H. F. Chen, photograph and biography not available at the time of publication.

J. M. Liu, photograph and biography not available at the time of publication.

P. Davis, photograph and biography not available at the time of publication.

T. Aida, photograph and biography not available at the time of publication.